OXFORD

International Journal of Neuropsychopharmacology (2019) 22(9): 548–559

doi:10.1093/ijnp/pyz036
Advance Access Publication: August 1, 2019
Regular Research Article

REGULAR RESEARCH ARTICLE

Association Between Reduced Brain Glucose Metabolism and Cortical Thickness in Alcoholics: Evidence of Neurotoxicity

Dardo G. Tomasi, Corinde E. Wiers,Ehsan Shokri-Kojori, Amna Zehra, Veronica Ramirez, Clara Freeman, Jamie Burns, Christopher Kure Liu, Peter Manza, Sung W. Kim, Gene-Jack Wang, Nora D. Volkow

National Institute on Alcohol Abuse and Alcoholism, Bethesda, MD (Dr Tomasi, Dr Wiers, Dr Shokri-Kojori, Ms Zehra, Ms Ramirez, Ms Freeman, Ms Burns, Mr Kure Liu, Dr Manza, Dr Kim, Dr Wang, and Dr Volkow); National Institute on Drug Abuse, Bethesda, MD (Dr Volkow).

Correspondence: Dardo Tomasi, PhD, 10 Center Dr, Rm B2L124, Bethesda, MD 20892-1013 (dardo.tomasi@nih.gov).

Abstract

Background: Excessive alcohol consumption is associated with reduced cortical thickness (CT) and lower cerebral metabolic rate of glucose (CMRGlu), but the correlation between these 2 measures has not been investigated.
Methods: We tested the association between CT and cerebral CMRGlu in 19 participants with alcohol use disorder (AUD) and 20 healthy controls. Participants underwent 2-Deoxy-2-[18F]fluoroglucose positron emission tomography to map CMRGlu and magnetic resonance imaging to assess CT.
Results: Although performance accuracy on a broad range of cognitive domains did not differ significantly between AUD and HC, AUD had widespread decreases in CT and CMRGlu. CMRGlu, normalized to cerebellum (rCMRGlu), showed significant correlation with CT across participants. Although there were large group differences in CMRGlu (>17%) and CT (>6%) in medial orbitofrontal and BA 47, the superior parietal cortex showed large reductions in CMRGlu (~17%) and minimal CT differences (~2.2%). Though total lifetime alcohol (TLA) was associated with CT and rCMRGlu, the causal mediation analysis revealed significant direct effects of TLA on rCMRGlu but not on CT, and there were no significant mediation effects of TLA, CT, and rCMRGlu.
Conclusions: The significant correlation between decrements in CT and CMRGlu across AUD participants is suggestive of alcohol-induced neurotoxicity, whereas the findings that the most metabolically affected regions in AUD had minimal atrophy and vice versa indicates that changes in CT and CMRGlu reflect distinct responses to alcohol across brain regions.

Keywords: alcoholism, brain glucose metabolism, cortical thickness, cognition

Introduction

Alcoholism is associated with significant brain neurotoxicity, which is a consequence of concomitant co-morbidities (head trauma, nutrition deficits, and hepatic dysfunction) but also reflects the direct effects of excessive alcohol consumption (Zahr and Pfefferbaum, 2017). Acute alcohol consumption has been shown to transiently reduce the metabolic rate of glucose (CMRGlu; a surrogate for neuronal activity) in the human brain (Volkow et al., 1990, 2006, 2008; Wang et al., 2000), and chronic

Received: April 1, 2019; **Revised:** June 12, 2019; **Accepted:** July 15, 2019

Significance Statement

Though studies have shown that alcoholics have significant cortical atrophy and lower brain glucose metabolism, which is a marker of brain function, there is significant variability in the magnitude of these effects across brain regions. It is also unclear whether the metabolic and morphological changes represent a common neurotoxic manifestation or distinct process in alcoholism. By correlating the effects of alcoholism on brain glucose metabolism and cortical thickness in the same participants, we found that whereas in some brain regions these measures are strongly correlated, consistent with alcohol neurotoxicity (i.e., middle cingulum), in others they are not (i.e., inferior and middle temporal gyri), suggesting distinct processes (i.e., use of alternative energy sources for metabolism).

excessive alcohol drinking leads to longer lasting decreases in CMRGlu (Volkow et al., 2015, 2017). The CMRGlu decreases associated with acute and chronic alcohol consumption could reflect alcohol-induced reductions in brain activity (by decreasing neuronal excitability) or the use of alternative brain energy sources (acetate or other ketones) during intoxication (Volkow et al., 2013). However, the longer lasting reduction in CMRGlu reported in alcoholics cannot be accounted solely on the basis of reliance on alternative brain energy substrates and might reflect alcohol-induced neurotoxicity due to oxidative stress or neuroinflammation (Haorah et al., 2008; Jhala and Hazell, 2011).

The loss of cortical gray matter (GM) in prefrontal, motor, and temporal cortices, insula, and anterior cingulum in alcoholism (Cardenas et al., 2007; Makris et al., 2008; Fein et al., 2009) has been a consistent finding in alcohol use disorder (AUD) (Pfefferbaum et al., 1992; Hommer et al., 2001; Chanraud et al., 2007; Demirakca et al., 2011; Le Berre et al., 2014). This cortical GM loss in people with AUD likely reflects reversible neurodegeneration (Crews et al., 2004; Bartsch et al., 2007), although there is also evidence of long-lasting neuropathology particularly in frontal regions (Volkow et al., 1997). Few studies have evaluated GM atrophy and brain glucose metabolism in the same AUD participants. In an early positron emission tomography (PET) and MRI study, we documented decreased CMRGlu and loss of GM volume in the frontal cortices and subcortical structures for 10 AUD participants compared with 10 controls (Wang et al., 1993). Another study in 31 AUD patients and 18 controls found reduced cingulate metabolism in association with atrophy as a function of increasing age (Adams et al., 1993). However, a study found prefrontal cortex hypometabolism in absence of cortical shrinkage in 17 AUD participants compared with 9 controls (Dao-Castellana et al., 1998). A more recent PET-MRI study that used voxel-based morphometry (VBM) showed GM volume loss and reduced glucose metabolism in the cerebellum, thalamus, hippocampus, and parahippocampal gyrus as well as in cingulate, dorsolateral, premotor, and parietal cortices in 17 alcoholic patients studied during early abstinence compared with 16 controls (Ritz et al., 2016). None of these studies, however, assessed cortical thickness (CT). Whereas reduced GM volume could reflect reductions in surface area, CT, or both, no PET-MRI study, to our knowledge, has documented the correlation between CT or surface area with CMRGlu in AUD participants. Also, though partial volume effects (PVE) secondary to cortical atrophy could explain the reduced CMRGlu in alcoholics, none of these PET-MRI studies corrected glucose metabolism for PVE.

In the present study, we aimed to assess the association between CMRGlu, CT, and GM volume in AUD participants and healthy controls (HC) using PET with 2-Deoxy-2-[18F] fluoroglucose (FDG) to measure brain glucose metabolism, after correcting for PVE, and surface-based analyses of MRI structure to measure CT. We hypothesized that CMRGlu, CT, and GM volume would be lower for AUD than for HC, that lower CT or GM volume would correlate with reduced CMRGlu in AUD, and that PVE corrections would not have a major impact in the group differences in glucose metabolism.

Materials and Methods

Participants

A group of 19 individuals with AUD and 20 HCs participated in the study. The 2 groups did not differ in age, gender proportion, or body mass index (Table 1). Participants were screened to exclude major medical, neurological, and psychiatric disorders, head trauma (with loss of consciousness longer than 30 minutes), chronic use of psychoactive medications, current or past diagnosis of substance use disorder (other than alcohol abuse and/or dependence in the AUD group, or current tobacco smoking in either group) as assessed by the Structured Clinical Interview for the Diagnostic and Statistical Manual of Mental Disorders (American Psychiatric Association, 2000), and metallic implants, which are contraindicated for MRI. Women were neither pregnant nor breastfeeding and were studied in the mid-follicular phase (3–10 days after the first day of their last period). AUD participants had at least 5 years' history of heavy drinking and were abstinent from alcohol 3.8 days at the time of the scans (range 0–7 days). All participants had a negative urine drug screen on the days of testing and were free of psychoactive medications within 24 hours of study procedures (except for 1 AUD participant who used benzodiazepines [oxazepam, 15 mg] for detoxification on the day of study). All participants provided written informed consent to participate, which was in accordance with the Declaration of Helsinki and approved by the Institutional Review Board at the National Institutes of Health (Combined Neurosciences White Panel).

On the day of screening (first study day), participants completed the Alcohol Use Disorders Identification Test (AUDIT) as a measure of harmful alcohol consumption, the Timeline Follow-back to assess daily alcohol consumption in the 90 days prior to the study, the Lifetime Drinking History to assess total lifetime alcohol consumption (TLA), the Alcohol Dependence Scale to assess the severity of dependence, the Wechsler Abbreviated Scale of Intelligence subtests Matrix Reasoning and Vocabulary as a proxy for general intelligence, the State-Trait Anxiety Inventory, the Obsessive Compulsive Drinking Scale to assess alcohol craving, and the Beck Depression Inventory to assess depression symptoms. The Clinical Institute Withdrawal Assessment for Alcohol (CIWA) was used to assess alcohol withdrawal symptoms. The AUD participants remained in the NIH's clinical center overnight to ensure that they did not ingest any alcohol and were scanned on the following study day with both MRI and PET.

Table 1. Participant Characteristics

	AUD (n = 19) (mean ± SD)	HC (n = 20) (mean ± SD)	P value[a]
Demographics			
Age (years)	47.6 ± 10.1	46.8 ± 10.5	NS
Gender (males/females)	14/5	13/7	NS
Height (m)	1.72 ± 0.09	1.70 ± 0.12	NS
Weight (kg)	79 ± 15	83 ± 16	NS
Education (years)	12.4 ± 2.9	15.2 ± 2.4	0.002
Smokers/no smokers	10/9	0/20	<1E-04
Premorbid cognition and psychiatric symptoms			
WASI-II Intelligence (IQ)	90 ± 16	103 ± 16	0.02
STAI anxiety	39 ± 12	29 ± 8	0.001
OCDS obsessive	4.4 ± 4.1	0.2 ± 0.7	2E-04
OCDS compulsive	7.7 ± 5.1	0.7 ± 1.3	9E-06
Depression	7.8 ± 9.9	1.3 ± 1.6	0.01
Alcohol use			
TLFB (average drinks per day/90 days)	10.6 ± 6.5	0.8 ± 1.0	4E-06
Maximum CIWA score	2.2 ± 3.2	0.2 ± 0.6	0.03
AUDIT total score	21.6 ± 8.4	1.6 ± 1.7	3E-09
Alcohol dependence	13 ± 7	0.2 ± 0.4	1E-08
Years of alcohol use	30 ± 11	26 ± 14	NS
Average frequency (drinking days/month)	25 ± 7	2 ± 3	2E-12
Average quantity (drinks/drinking day)	12 ± 9	2 ± 1	1E-04
Days since last drink	3.8 ± 2.3	2580 ± 3880	0.006
Brain volume			
Cortical GM (% of ICV)	35 ± 5	37 ± 4	NS
White matter (% of ICV)	36 ± 5	37 ± 5	NS
Subcortical GM (% of ICV)	4.5 ± 0.7	4.5 ± 0.7	NS
Ventricles (% of ICV)	2.3 ± 0.8	1.9 ± 0.6	NS
Cerebellum (% of ICV)	10.4 ± 1.6	10.3 ± 0.8	NS
ICV (mL)	1252 ± 231	1283 ± 228	NS

Abbreviations: AUD, alcohol use disorder; AUDIT, Alcohol Use Disorders Identification Test; CIWA, Clinical Institute Withdrawal Assessment; HC, healthy control; GM, gray matter; ICV, intracranial volume; IQ, intelligence quotient; OCDS, Obsessive Compulsive Drinking Scale; STAI, State-Trait Anxiety Inventory; TLFB, Timeline Follow-back; AUDIT; WASI-II, Wechsler Abbreviated Scale of Intelligence.
[a]*P* values are from unpaired *t* test or χ^2 test.

Cognitive Battery

The Cambridge Neuropsychological Test Automated Battery was used to assess delay aversion, set-shifting processing, psychomotor speed, pattern recognition, reaction time, spatial planning, working memory capacity, response inhibition, and spatial working memory (Robbins et al., 1994). The battery was selected to cover a broad range of cognitive abilities within a brief time period.

PET

Participants were asked to fast (except drinking water) for at least 4 hours prior to the PET imaging session, which was performed using a high-resolution research tomograph (Siemens AG) with a 2.5-mm isotropic point spread function. Venous catheters were placed in the antecubital vein for radiotracer injection and in the dorsal hand vein for arterialized blood sampling (arterialization was achieved by warming the hand to 44–50°C) to measure the concentration of radioactivity in plasma (every minute from 1–10 minutes and then at 15, 20, 30, 40, 50, 60, and 75 minutes after FDG injection). Attenuation correction was based on a transmission scan obtained with a 137-Cesium rotating pin source. Commercially manufactured FDG (8 mCi) was injected i.v. over a period of 1 minute. Emission scans with approximately 2.5-mm isotropic resolution were obtained using 3D list mode starting immediately after FDG injection and continued for 75 minutes. Fasting glucose levels were measured prior to FDG injection, 30 minutes after injection, and at the end of the PET scan. During the PET imaging procedures, the participants rested quietly under dim illumination and minimal acoustic noise. Participants were asked to keep their eyes open and were monitored throughout the procedure. During the PET scan, a cap with small light reflectors was placed on the participant's head to monitor head position with a Polaris Vicra head tracking system (Northern Digital Inc.). Information about the head movement was used in the PET image reconstruction process to correct for motion-related image blurring (Olesen et al., 2013). The PET raw data were reconstructed with a 3D-ordered subset expectation maximization algorithm to generate 45 frames of data for each participant (temporal resolution for all 45 frames = 100 seconds).

Voxelwise CMRGlu was computed in PMOD v3.4 (PMOD Technologies, Zurich, Switzerland) based on an autoradiographic solution for the 2-tissue compartment model up to the mid-time of the summary image (55 minutes). The CMRGlu maps in μmol/100 mL/min were aligned to the participant's structural MRI and then normalized to the Montreal Neurological Institute template with 2-mm isotropic resolution using the linear image registration tool (FLIRT) of the FSL software library (version 5.0; http://www.fmrib.ox.ac.uk/fsl) (Jenkinson et al., 2002). CMRGlu was corrected for PVE with a voxel-wise approach using the Müller-Gärtner method (Müller-Gärtner et al., 1992) implemented in the PETPVE12 toolbox (Gonzalez-Escamilla et al., 2017). The statistical parametric mapping software (SPM12; Wellcome Trust Centre for Neuroimaging, London, UK) was used

to segment the MP-RAGE images into GM, white matter, and cerebrospinal fluid, which were used to correct the PET images for PVE.

Regions-Of-Interest (ROI) Analyses

The CMRGlu values were averaged within each of the 68 cortical and 18 subcortical GM parcels from FreeSurfer (see below).

Pharmacokinetic Modelling

A 2-tissue compartment model with $k_4=0$ (i.e., neglecting FDG-6-PO dephosphorylation) was used to assess the average rates of uptake, K_1, clearance, k_2, and phosphorylation, k_3, within each of the 68 cortical GM partitions in the Desikan-Killiany atlas (Desikan et al., 2006) and 18 subcortical GM partitions (Fischl et al., 2002). We assumed a blood volume fraction, $\nu=4\%$ (Leenders et al., 1990), and that the activity at each voxel,

$$C(t) = (1-\nu)(C_1(t) + C_2(t)) + \nu C_p(t) \quad (1)$$

reflects the concentrations of FDG in arterial plasma, $C_p(t)$, and in the reversible, $C_1(t)$, and irreversible, $C_2(t)$, compartments that are given by the system of differential equations:

$$\begin{cases} \frac{dC_1(t)}{dt} = K_1 C_p(t) - (k_2 + k_3) C_1(t) \\ \frac{dC_2(t)}{dt} = k_3 C_1(t) \end{cases}$$

The Levenberg-Marquardt algorithm for nonlinear least squares fitting (Press et al., 1992) was used to fit Eq. (1) to the experimental data (C_p and C) with 3 adjustable parameters (K_1, k_2, and k_3). The Livermore solver for ordinary differential equations (Hindmarsh, 1980) was used to solve Eq. (2) in terms of $C_p(t)$ and calculate $C_1(t)$ and $C_2(t)$. The 2-tissue compartment modeling described above (Tomasi et al., 2017) was implemented using the Interactive Data Language (IDL, ITT Visual Information Solutions, Boulder, CO).

MRI

Immediately after the PET scans the participants underwent MRI on a 3.0T Magnetom Prisma scanner (Siemens Medical Solutions USA, Inc., Malvern, PA) equipped with a 20-channel head coil. T1-weighted 3D magnetization-prepared gradient-echo (MP-RAGE, TR/TE=2200/4.25 ms; FA=9°, 1-mm isotropic resolution) and T2-weighted spin-echo multi-slice (TR/TE=8000/72 ms; 1.1 mm in-plane resolution; 94 slices, 1.7-mm slice thickness; matrix=192) pulse sequences were used to acquire high-resolution anatomical brain images.

The minimal preprocessing pipelines (Glasser et al., 2013) of the Human Connectome Project were used for spatial normalization of the structural scans to the stereotactic space of the Montreal Neurological Institute. The FreeSurfer pipeline implemented by the Human Connectome Project was used to compute the pial and white matter surfaces, segment the anatomical MRI scans into 68 cortical and 18 subcortical GM ROIs, and estimate the average CT and surface area for each of the cortical partitions in the Desikan-Killiany atlas (Desikan et al., 2006).

Statistical Analyses

CMRGlu values had considerable intersubject variability, which decreased the sensitivity for detecting group differences in CMRGlu. Since the cerebellum did not show significant group differences in CMRGlu (see Results), relative CMRGlu (rCMRGlu) maps, normalized to the average CMRGlu in cerebellum, were computed to reduce the coefficient of variation (C_v) of the metabolic measures across participants.

Voxelwise ANCOVA, implemented in SPM12 with group membership as a factor and age and education as covariates of no interest, was used to test for group differences in GM volume and rCMRGlu. Voxelwise ANCOVA was also used to assess the effects of group and CT on rCMRGlu using age and education as covariates of no interest. Statistical inference based on a familywise error (FWE) rate was implemented to control for false positives in voxelwise analyses. Specifically, clusters were considered statistically significant if they had an FWE-corrected $P_{FWE}<.05$, using a cluster-defining threshold $P=.005$ and a minimum cluster size of 100 voxels.

ANCOVA was also used to assess main effects and interactions effects on rCMRGlu for the ROI analyses. The ANCOVA model included 2 groups (HC and AUD), CT as a covariate of interest, and 2 covariates of no interest to control for group differences in education- and age-related declines in rCMRGlu and CT (Volkow et al., 2000; Raz, 2006). In addition, ANCOVA was used to control for the effects of gender, education, and tobacco smoking while preserving an adequate level of statistical power for the small sample in this study. The statistical group differences in CT and the correlations between rCMRGlu and CT across participants were corrected for multiple comparisons using a false discovery rate (FDR) correction for 86 (rCMRGlu) or 68 (CT) ROIs. To highlight regional differences for group comparisons in rCMRGlu, we set more stringent criteria using Bonferroni correction for 86 ROIs.

Mediation Analysis

We tested if the effect of excessive alcohol use on CT was mediated by the changes in rCMRGlu or whether the decreases in rCMRGlu were mediated by the changes in CT using causal mediation analysis implemented in R (http://CRAN.R-project.org/package=mediation). We first fitted a mediator model where the average CT across all cortical ROIs was modeled as a function of the average rCMRGlu in cortical ROIs, or vice versa, and included age and education as covariates in the model. One-thousand simulations with a quasi-Bayesian Monte Carlo method based on a normal approximation (Imai et al., 2010) and a heteroskedasticity-consistent estimator for the covariance matrix (Zeileis, 2006) were used to calculate the uncertainty estimates.

Results

Demographic and Alcohol Use Variables

Ten AUD participants but none of the HC participants were current tobacco smokers ($\chi2=13.9$, $P<.0001$; Table 1). On average, AUD participants consumed 136 g/d alcohol during the last 90 days. Conversely, 8 of the HC participants had no alcohol intake during the last 90 days, and the remainder consumed an average of 27 g/d alcohol. On the study day, AUD participants had an average CIWA score of 2.2±3.3. The AUDIT score was <6 for all HCs and >6 for all AUD participants (Table 1). AUD participants had a lower intelligence quotient ($P=.03$) and fewer years of education ($P<.001$) than HCs. Depression (Beck Depression Inventory score) and anxiety (State-Trait Anxiety Inventory score) symptom ratings and alcohol craving (obsessive and compulsive Obsessive Compulsive Drinking Scale scores) and

withdrawal (CIWA score) were higher for AUD than for HCs (Table 1). For 1 AUD participant who presented with severe withdrawal symptoms (i.e., nausea, vomiting, tremor, severe headache, disorientation, etc.; CIWA = 12) at arrival, oxazepam 15 mg was administerd during 2 days and discontinued 2 hours prior to the PET scan study.

Cognitive Measures

Cognitive performance did not differ significantly between AUD and HCs for any of the cognitive domains assessed with the Cambridge Neuropsychological Test Automated Battery.

Brain Morphometry

The intracranial volume (ICV) and the volumes of white matter and GM estimated from FreeSurfer ROI's tended to be smaller and the ventricles larger in AUD than HCs, but these differences were not significant (Table 1). In contrast, measures of CT were significantly lower for AUD (average 2.39 ± 0.10 mm) than for HCs (average 2.50 ± 0.12 mm; $P = .005$, t test). CT decreases encompassed the whole cortex, reaching a maximum of 5% in dorsolateral prefrontal cortex, superior motor cortex, and temporal pole. Smaller CT decreases were found in the insula, occipital, and posterior parietal regions (<3%; Figure 1A).

The ROI analyses revealed lower CT for AUD than for HCs in frontal regions (paracentral, lateral, and medial orbitofrontal; rostral middle frontal; and pars orbitalis), supramarginal, entorhinal, and fusiform gyri ($P < .004$, FDR-corrected; Figure 1B; supplementary Table 1). In contrast, group differences in surface area were not significant for any ROI.

The VBM analysis in this study (see supplementaty information for the VBM methodology and results) showed lower GM volume for AUD than for HCs, predominately in prefrontal and parietal cortices, which did not reach statistical significance in any brain region after FWE corrections for multiple comparisons (supplementary Figure 1). ICV did not show significant correlation with CT or GM volume in any brain region.

Pharmacokinetics and Glucose Metabolism

FDG plasma concentration did not differ between groups ($P > .05$; Figure 2A). The group difference in blood glucose level was not significant (AUD: 87 ± 10 mg/dL; HC: 84 ± 5 mg/dL; $P = .2$). The regional time-activity curves differed significantly between the groups. Specifically, in cortical ROIs, AUD showed lower activity than HCs (Figure 2B) for $t > 20$ minutes after tracer injection ($P < .05$). Compared with HCs, the AUD's lower time-activity in cerebellum did not reach significance at any time point. The 2-tissue compartment model accurately fitted the data in all ROIs (supplementary Figure 2) and revealed lower phosphorylation rate (k_3) in 53/86 cortical and subcortical ROIs in AUD compared to HC ($P < .05$, FDR-corrected; Figure 2C). The group differences in the rates of uptake (K_1) and clearance (k_2), however, did not differ for any ROI.

The whole-brain average CMRGlu was lower for AUD (33.7 ± 4.3 μmol/100g/min) than for HCs (39.1 ± 6.0 μmol/100g/min; $P = .002$, t test). The CMRGlu in cerebellar cortex did not differ between groups (AUD: 27.3 ± 3.9 μmol/100g/min; HC: 27.2 ± 5.0 μmol/100g/min; $P = .93$). The C_V of the whole-brain average CMRGlu was 0.15 for HCs and 0.13 for AUD. Since group differences in CMRGlu were not significant in any cerebellar

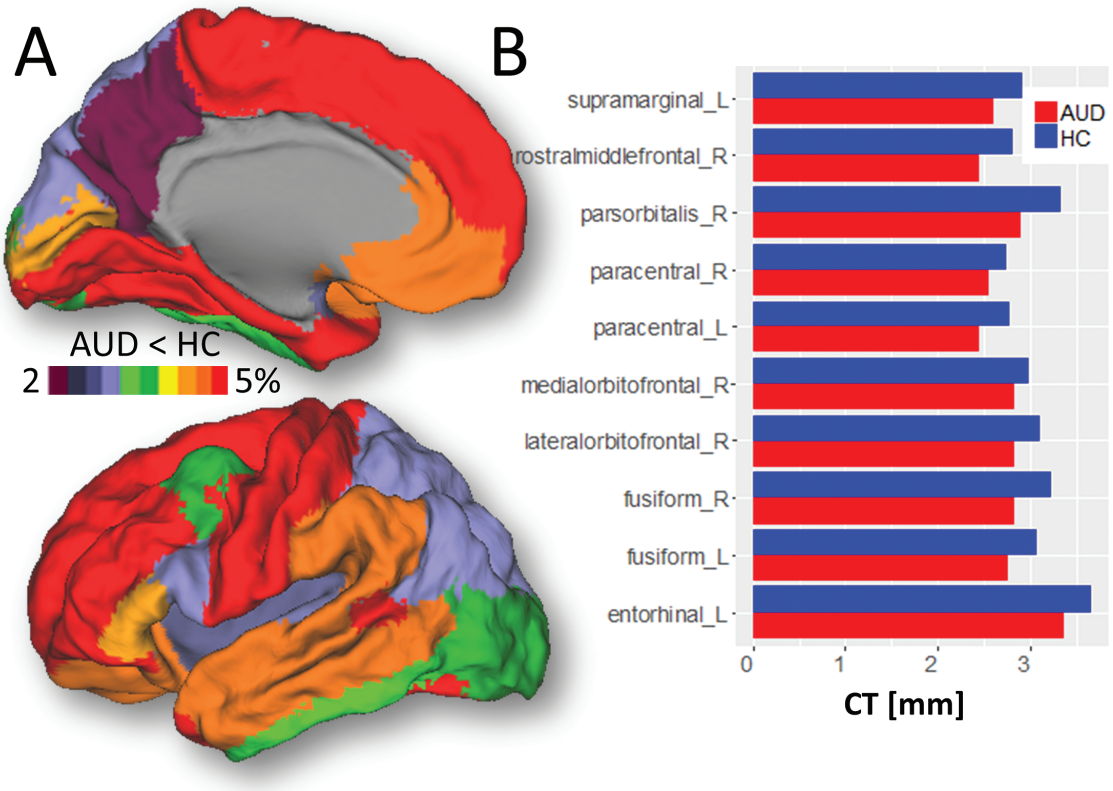

Figure 1. Cortical thickness (CT). (A) FreeSurfer regions of interest (ROI) analyses showing average group differences in CT superimposed on the medial (top) and lateral (bottom) surface views of the PALS-B12. (B) Bar plots showing ROI-averages of CT across alcohol use disorder (AUD) and healthy control (HC) participants. Model: ANCOVA. Significance: $P < .05$, FDR-corrected. Sample size: 19 AUDs and 20 HCs.

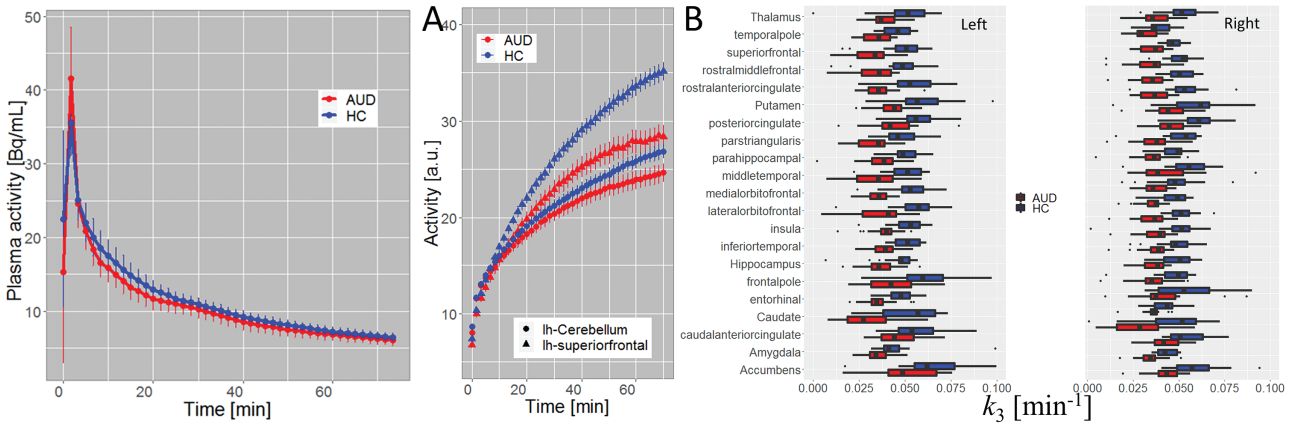

Figure 2. FDG-Pharmacokinetics. (A) Comparison of the arterial plasma samples, interpolated to 100-s intervals, showing that differences in plasma activity between alcohol use disorder (AUD) and healthy control (HC) were not statistically significant. (B) Average time-activity curves in left cerebellum and a cortical region (left superior frontal gyrus) for AUD and HC participants. (C) Bilateral regions of interest (ROIs) showing statistically significant group differences in the phosphorilation rate of 2-Deoxy-2-[18F]fluoroglucose (FDG) (k_3) ($P < .05$, FDR-corrected) computed using the 2-tissue compartment model (see text).

region, we used the whole cerebellum as a control region to normalize CMRGlu for subsequent analyses. The relative CMRGlu (rCMRGlu) had lower variability than CMRGlu ($C_V = 0.09$ for HC and 0.11 for AUD), which enhanced the statistical power for detecting group differences in glucose metabolism.

Figure 3A shows the average pattern of rCMRGlu for representative AUD and HC participants. Anatomical ROI analyses based on average rCMRGlu values within the GM partitions showed lower rCMRGlu in 23/86 ROIs (Figure 3B–C; supplemental Table 2) for AUD than for HCs. Specifically, compared with HCs, cortical rCMRGlu reductions in AUD participants were most pronounced in primary and association auditory areas (banks of the superior temporal sulcus ["bankssts"], transverse and superior temporal gyri); language (supramarginal gyrus, pars opercularis, and orbitalis); motor and premotor areas (precentral and postcentral gyri); lateral orbitofrontal, rostral middle frontal, isthmus, and rostral anterior cingulate; inferior and superior parietal; and entorhinal cortices and cuneus ($P < 7E-04$, Bonferroni-corrected; ANCOVA1 and ANCOVA2), with group differences as high as 18%. Compared with uncorrected images, PVEc increased 4.6 ± 1.0% the rCMRGlu across participants and ROIs, an effect that did not differ between HCs and AUD ($P = .8$; t test) and did not alter the group differences in rCMRGlu (supplementary Figure 2). The whole-brain average CMRGlu did not differ significantly for the AUD participant imaged under the effect of benzodiazepines (CMRGlu = 31μmol/100g/min) and the rest of the AUD participants (23 < CMRGlu < 43μmol/100g/min). The removal of this participant from the analysis did not alter the group differences in rCMRGlu.

Voxelwise ANCOVA revealed lower rCMRGlu for AUD than HCs. These group differences were overall greater for lateral than for midline regions and most prominent in temporal and occipital cortices, pars triangularis, and Rolandic operculum ($P < .05$, FWE-corrected; Figure 3D; Table 2).

Cortical Thickness vs Glucose Metabolism

Among ROIs that showed large group differences in CT (>6%), the right medial orbitofrontal, and pars orbitalis (BA 47) also showed the largest group differences in CMRGlu (>17%), whereas, the left entorhinal and right transverse temporal ROIs demonstrated the smaller group differences in CMRGlu (<12%). Similarly the superior parietal region, which showed one of the largest group differences in CMRGlu (~17%) had minimal differences in CT (~2.2%).

The voxelwise analyses showed significant correlations between rCMRGlu and CT across AUD participants ($R = 0.6$; $P = .006$) and a trend across HC participants ($R = 0.42$; $P = .06$). Specifically, ANCOVA revealed that decreases in CT were associated with decreases in rCMRGlu in inferior and middle occipital, fusiform, and inferior frontal gyri, superior temporal pole, inferior frontal operculum, precuneus, and middle cingulum ($P < .05$, FWE-corrected; Figure 4A; Table 2) and a CT × group interaction on rCMRGlu such that the slope of the CT-related increases in rCMRGlu in superior medial frontal gyrus was steeper for AUD than for HCs ($P < .05$, FWE-corrected; Table 2).

The ROI analyses confirmed the voxelwise analyses. Specifically, across all participants, the correlation between rCMRGlu and CT was strongest in superior temporal sulcus ($R = 0.7$) and also significant in parietal, temporal, and frontal cortices and in fusiform gyrus ($R > 0.5$; $P < .05$, FDR-corrected; Figure 4B–C). In AUD participants, the correlation between rCMRGlu and CT was strongest bilaterally in caudal middle frontal gyrus ($R = 0.73$; $P = 4E-04$) and also significant in precentral, superior, and rostral middle frontal gyri, pars triangularis, and superior temporal sulcus ($R > 0.57$; $P < .05$, FDR-corrected). In controls, the correlation between rCMRGlu and CT was strongest bilaterally in the superior temporal sulcus ($R = 0.68$; $P = 0.001$) and also significant in fusiform, superior, and inferior parietal, inferior, middle, and superior temporal gyri ($R > 0.57$; $P < .05$, FDR-corrected). The scatter plots in Figure 4C highlight the correlations between CT and rCMRGlu in prefrontal regions for AUD and HC participants. PVEc did not change the associations between CT and rCMRGlu (supplementary Figure 3). The regression plots on Figure 4C also revealed that for an equivalent CT value, rCMRGlu were lower for AUD participants than for HC.

Alcohol Usage Variables vs Cortical Thickness and CMRGlu

ANCOVA with the logarithm of TLA as a covariate of interest revealed significant decreases in CT and rCMRGlu with greater TLA ($F > 8.3$; $P < .007$) such that the group differences in CT and rCMRGlu were explained by group differences in TLA ($F = 8.0$, $P = .008$). Other alcohol use variables (i.e., Timeline Follow-back: total drinks in past 90 days, AUDIT total score, lifetime drinking

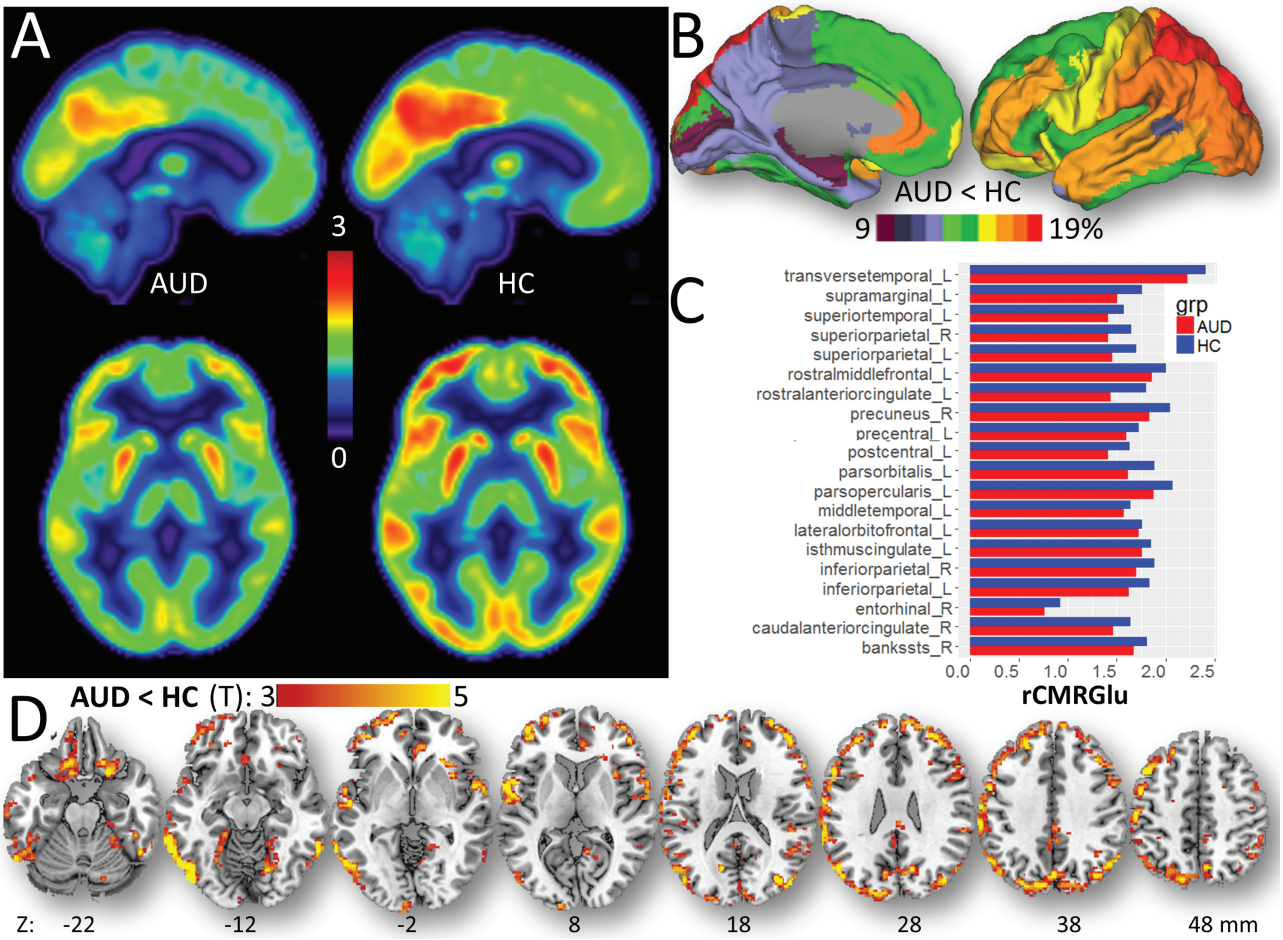

Figure 3. Relative glucose metabolism (rCMRGlu). (A) Mean cerebral metabolic rate of glucose, relative the cerebellum, in 19 alcohol use disorder (AUD) and 20 healthy control (HC) participants. (B) Average group differences in rCMRGlu within cortical FreeSurfer regions of interest (ROIs) rendered on lateral and medial surface views of the PALS_B12 template. (C) Bar plots showing statistically significant group differences in rCMRGlu within ROIs (Bonferroni corrected). (D) Statistical significance of the group differences in rCMRGlu overlaid on axial views of a brain template. Sample size: 19 AUDs and 20 HC. Statistical imaging threshold $P < .005$.

history: average number of drinks per occasion) had similar effects on rCMRGlu ($P < .003$) and CT ($P < .02$).

Mediation

The direct effects of the logarithm(TLA) on rCMRGlu (cortical mean) were significant ($P < .01$) but those on average CT were not ($P > .53$). The causal effects of TLA, CT, or rCMRGlu as mediators were not significant.

Discussion

This is the first study to assess the relationships between alcohol-drinking history, CT, and brain glucose metabolism in AUD participants. Compared with HCs, AUD participants without cognitive deficits had reduced CT and lower rCMRGlu, which was driven by a slower rate of phosphorylation (k_3) that was most prominent in frontal regions. Group comparisons also revealed brain regions with small changes in CT but marked reductions in rCMRGlu, such as the superior parietal lobes, as well as regions with small reductions in rCMRGlu but large changes in CT, such as the left paracentral gyrus. Across participants, rCMRGlu was significantly correlated with CT, independently for HCs and AUD. However, for regions with similar CT in both groups, the CMRGlu tended to be lower in AUD participants than in HC participants. Alcohol use history and AUD symptom severity explained 25% of the variance in CT and cortical rCMRGlu but without rCMRGlu-mediation effects on CT or without CT-mediation effects on CMRGlu, which suggests that distinct factors contribute to the decreases in CT and rCMRGlu in AUD.

The AUD group showed lower CMRGlu in widespread cortical regions compared with HC, and the history of alcohol use was associated with decreased glucose metabolism such that increased TLA was associated with decreased rCMRGlu. These findings are consistent with prior studies showing reductions in brain glucose metabolism in alcoholism (Adams et al., 1993; Wang et al., 1993; Dao-Castellana et al., 1998; Wang et al., 2000, 2003; Volkow et al., 2006, 2008, 2013, 2015; Ritz et al., 2016). We have previously interpreted the CMRGlu decreases in AUD as reflecting alcohol-induced reductions in neuronal activity, the use of alternative energy sources by the brain and/or neurotoxicity from excessive alcohol use (Volkow et al., 2013). In the current work, we assessed whether decreased CMRGlu reflected neurotoxicity, as evidenced by cortical atrophy in AUD individuals (Haorah et al., 2008; Jhala and Hazell, 2011). In vitro studies have shown that alcohol can increase lipid peroxidation, which suggested that oxidative stress might be a mechanism by which alcohol induces neurodegeneration (Haorah et al., 2008).

Table 2. Spatial Coordinates in the MNI Space and Statistical Information for Clusters Showing Significant Group Differences in rCMRGlu Between AUD and HC Participants, Linear Effects of CT on rCMRGlu, and CT by Group Interactions on rCMRGlu

Brain region	BA	MNI coordinates (mm)			Cluster size	AUD < HC (t-score)	CT (t-score)	
		x	y	Z	(voxels)		AUD & HC	AUD > HC
AUD < HC								
Middle temporal	37	−66	−48	−12	1126	7.0	n.s.	n.s.
Inferior temporal	37	−58	−64	−10		5.8	n.s.	n.s.
Inferior occipital	19	−46	−78	−12		5.0	n.s.	n.s.
Middle occipital	39	36	−76	16	379	5.1	n.s.	n.s.
Middle occipital	39	48	−78	20		5.1	n.s.	n.s.
Cuneus	19	6	−84	34		4.7	n.s.	n.s.
Pars triangularis	44	56	20	22	764	4.6	1.8	n.s.
Rolandic operculum	48	60	−8	10		4.4	2.0	n.s.
Sup temporal pole	38	56	4	4		4.4	2.2	n.s.
CT								
Inferior occipital	19	−28	−82	−12	9401	n.s.	6.6	n.s.
Sup temporal pole	38	−54	4	0		3.3	6.5	n.s.
Fusiform	18	−24	−76	−16		n.s.	6.4	n.s.
Middle occipital	39	40	−80	16	9291	3.3	6.3	n.s.
Middle Frontal	45	44	32	30		n.s.	5.8	n.s.
Inferior frontal operculum	44	52	12	14		n.s.	5.8	n.s.
Middle cingulum	23	8	−46	36	2047	2.5	6.1	n.s.
Middle cingulum	23	6	−14	42		n.s.	5.4	n.s.
Precuneus	5	8	−38	56		n.s.	5.2	n.s.
CT × group								
Superior med frontal	32	8	40	40	46	n.s.	n.s.	4.5

AUD, alcohol use disorder; BA, Brodmann area; CT, cortical thickness; FWE, familywise error; HC, healthy control; rCMRGlu, relative cerebral metabolic rate of glucose. Sample: 19 AUD and 20 HC participants. Model: ANCOVA with age and education covariates of no interest. Statistical threshold: $P < .05$, FWE-corrected. The *t* scores correspond to peak cluster-level statistics (bold values; FWE-corrected) or voxel-level statistics (not bold values; uncorrected).

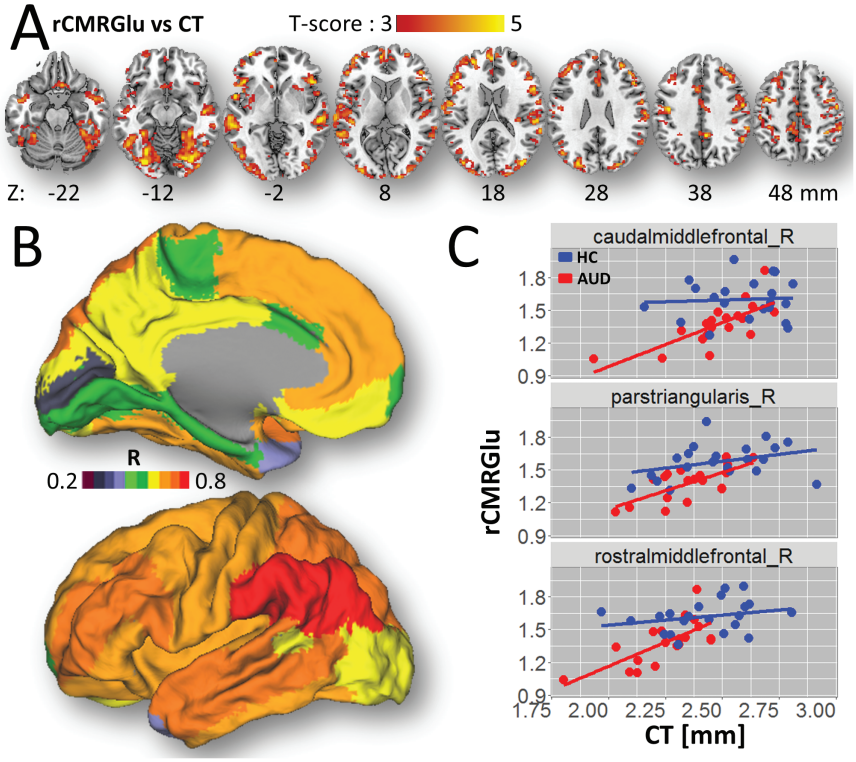

Figure 4. rCMRGlu-cortical thickness (CT) association. (A) Statistical significance of the effect of CT-related increases in relative glucose metabolism (rCMRGlu). (B) FreeSurfer regions of interest (ROI) analyses showing the correlation factors between rCMRGlu and CT within the anatomical partitions overlaid on medial and lateral surface views of the PALS-B12 template. (C) Scatter plots showing this association for 3 representative frontal ROIs for alcohol use disorder (AUD) participants and healthy controls (HC). Statistical model: ANCOVA with age as a covariate of no interest. Statistical imaging threshold of $P < .005$.

Oxidative stress and neuroinflammation have been linked to reduced brain glucose metabolism in neurodegenerative diseases such as Alzheimer's disease, traumatic brain injury, and aging (Daulatzai, 2017). Proton magnetic resonance spectroscopy studies have reported lower levels of brain N-acetylaspartate, a marker of neuronal integrity, in alcohol users (light and heavy drinkers) compared with controls (Jagannathan et al., 1996; Bendszus et al., 2001; Schweinsburg et al., 2001; Meyerhoff et al., 2004; Silveri et al., 2014), and postmortem studies have reported neuronal loss in the frontal lobes in AUD (Harper et al., 1985, 1987), which are consistent with evidence of neurotoxicity in AUD.

Here we show a significant correlation between rCMRGlu and CT in prefrontal cortical regions, pars triangularis (BA 45) and inferior parietal cortices in AUD participants but less so in HCs. Moreover, compared with HCs, the AUD group demonstrated a widespread reduction in CT predominantly in frontal lobe regions but also in fusiform gyrus and medial temporal cortex. The AUD's reduced CT is also consistent with prior studies (Durazzo et al., 2011; Fortier et al., 2011; Momenan et al., 2012; Durazzo et al., 2013; Bae et al., 2016) and supports the notion that chronic excessive alcohol consumption can damage the brain (Henderson et al., 2018), even in AUD indiviudals with normal cognitive performance and no medical co-morbidities. The reduction in CT was associated with the severity of alcohol consumption, such that CT decreased with increased TLA. Intriguingly, the mediation analyses showed that TLA did not significantly mediate the CT in the present study, whereas it showed significant mediation of hypometabolism.

The large CMRGlu decreases and minimal CT deficits in the superior parietal cortex of the AUD participants suggest that this brain region might have a higher reliance on alternative energy sources (i.e., acetate), thus driving the large group differences in metabolism (Volkow et al., 2013). In contrast, the paracentral gyrus may predominantly rely on CMRGlu, which could help explain why it showed minimal changes in metabolic activity despite its marked decreases in CT in AUD.

The absence of significant group differences in CMRGlu in the cerebellum contrasts with our prior findings of pronounced metabolic decreases after acute alcohol administration in the cerebellum (Volkow et al., 2013). During alcohol intoxication, the cerebellum and other brain regions may rely on acetate as a substrate for energy production (Volkow et al., 2013). Thus, the cerebellum may show low CMRGlu during alcohol intoxication, when the level of plasma acetate concentration is high as in our prior study, but not during alcohol abstinence, when the level of plasma acetate concentration is low as in this study.

We did not detect significant group differences in cortical surface area, in agreement with previous work (Durazzo et al., 2011). In contrast to previous studies, we did not find associations between the severity of alcohol consumption and CT (Fein et al., 2002; Thayer et al., 2016; Lange et al., 2017), nor did we find significant group differences in GM volume (Fein et al., 2002, 2009; Cardenas et al., 2007; Chanraud et al., 2007; Mechtcheriakov et al., 2007; Makris et al., 2008), which may reflect the small sample size in our study. The fact that we found significant group differences in CT but not in GM volume suggests that alcohol's effects might be greater for CT than for GM volumes and/or that the GM volume effects might be less consistent across participants than those for CT. However, the small samples size of our study might have increased the chances of type II error in our volumetric measues. Specifically in our study, though not significant, the cortical volumetric measures in AUD were smaller than in HCs; but a sample of 30 AUD and 30 HCs for the same effect size ($r = 0.54$) would have been significant ($P < .05$, FWE-corrected). The differences in CT and CMRGlu in our AUD group might also reflect the effects of tobacco smoking and/or the interaction of alcohol and tobacco, which was characteristic of AUDs only.

Notably, there were no apparent effects on cognition, or if there were effects they were nondetectable by the standard battery we used in our study. The fact that we documented lower CT and CMRGlu in AUD participant with no medical comorbidities and who showed no evidence of cognitive impairment indicates that excessive alcohol consumption by itself might have deleterious effects to the brain that are not necessarily paralleled by deficits on traditional neurocognitive tests.

Limitations include the small sample size of the study, yet despite this, we were able to document significant effects of alcohol on CT and CMRGlu. Nonetheless, the small sample size limited our ability to address potential gender or age interaction effects. Furthermore, with its cross-sectional design, the study cannot assess if deficits in CT might have preceded alcohol initiation in these participants. However, the negative association between CT and the severity of alcohol consumption suggests this is not the case. PET was done in a condition of acute withdrawal (3.8 days since last drink), so the PET results might include changes related to craving rather than pure effects of chronic alcohol consumption per se, and our analysis indicates a partial restoration of metabolism with greater duration of abstinence. This is consistent with prior findings on brain metabolic recovery with abstinence in alcoholics (Volkow et al., 1994). Interestingly, we did not observe an effect of abstinence on CT, suggesting that these changes might be longer lasting. In this regard, it would have been desirable to assess these participants at multiple time points and determine whether CT and glucose metabolism recover with protracted abstinence. Since prior studies have documented effects of tobacco use on cortical volume and/or thickness (Kühn et al., 2010; Duriez et al., 2014; Durazzo et al., 2018), the lack of balance in tobacco smoking can be seen as a limitation for this study. We used smoking as a nuisance covariate to partially control for this difference in the statistical analysis. However, because in this study smoking is a characteristic of AUDs only, we cannot separate the contribution of smoking and their interaction with AUD from the group differences on CT or CMRGlu.

In summary, here we document lower CT in AUD participants, which was most pronounced in frontal and parietal cortical regions and associated with reduced glucose metabolism. The associations of history of alcohol use with CT and rCMRGlu and the absence of mediation effects between rCMRGlu and CT suggest both common and unique factors driving the reduced rCMRGlu and CT. Whereas the decrease in CT is likely to reflect neurotoxicity in AUD, the reductions in cortical CMRGlu are likely to reflect alcohol-related neurotoxicity as well as the use of alternative energy sources for brain metabolism.

Supplementary Materials

Supplementary data are available at *International Journal of Neuropsychopharmacology (IJNPPY)* online.

Acknowledgments

This work was accomplished with support from the National Institute on Alcohol Abuse and Alcoholism (Y1AA-3009).

Statement of Interest

None.

References

Adams KM, Gilman S, Koeppe RA, Kluin KJ, Brunberg JA, Dede D, Berent S, Kroll PD (1993) Neuropsychological deficits are correlated with frontal hypometabolism in positron emission tomography studies of older alcoholic patients. Alcohol Clin Exp Res 17:205–210.

American Psychiatric Association (2000) Diagnostic and statistical manual of mental disorders: DSM-IV-TR. 4 edition. Washington, DC: American Psychiatric Association.

Bae S, Kang I, Lee BC, Jeon Y, Cho HB, Yoon S, Lim SM, Kim J, Lyoo IK, Kim JE, Choi IG (2016) Prefrontal cortical thickness deficit in detoxified alcohol-dependent patients. Exp Neurobiol 25:333–341.

Bartsch AJ, Homola G, Biller A, Smith SM, Weijers HG, Wiesbeck GA, Jenkinson M, De Stefano N, Solymosi L, Bendszus M (2007) Manifestations of early brain recovery associated with abstinence from alcoholism. Brain 130:36–47.

Bendszus M, Weijers HG, Wiesbeck G, Warmuth-Metz M, Bartsch AJ, Engels S, Böning J, Solymosi L (2001) Sequential MR imaging and proton MR spectroscopy in patients who underwent recent detoxification for chronic alcoholism: correlation with clinical and neuropsychological data. AJNR Am J Neuroradiol 22:1926–1932.

Cardenas VA, Studholme C, Gazdzinski S, Durazzo TC, Meyerhoff DJ (2007) Deformation-based morphometry of brain changes in alcohol dependence and abstinence. Neuroimage 34:879–887.

Chanraud S, Martelli C, Delain F, Kostogianni N, Douaud G, Aubin HJ, Reynaud M, Martinot JL (2007) Brain morphometry and cognitive performance in detoxified alcohol-dependents with preserved psychosocial functioning. Neuropsychopharmacology 32:429–438.

Crews FT, Collins MA, Dlugos C, Littleton J, Wilkins L, Neafsey EJ, Pentney R, Snell LD, Tabakoff B, Zou J, Noronha A (2004) Alcohol-induced neurodegeneration: when, where and why? Alcohol Clin Exp Res 28:350–364.

Dao-Castellana MH, Samson Y, Legault F, Martinot JL, Aubin HJ, Crouzel C, Feldman L, Barrucand D, Rancurel G, Féline A, Syrota A (1998) Frontal dysfunction in neurologically normal chronic alcoholic subjects: metabolic and neuropsychological findings. Psychol Med 28:1039–1048.

Daulatzai MA (2017) Cerebral hypoperfusion and glucose hypometabolism: key pathophysiological modulators promote neurodegeneration, cognitive impairment, and alzheimer's disease. J Neurosci Res 95:943–972.

Demirakca T, Ende G, Kämmerer N, Welzel-Marquez H, Hermann D, Heinz A, Mann K (2011) Effects of alcoholism and continued abstinence on brain volumes in both genders. Alcohol Clin Exp Res 35:1678–1685.

Desikan RS, Ségonne F, Fischl B, Quinn BT, Dickerson BC, Blacker D, Buckner RL, Dale AM, Maguire RP, Hyman BT, Albert MS, Killiany RJ (2006) An automated labeling system for subdividing the human cerebral cortex on MRI scans into gyral based regions of interest. Neuroimage 31:968–980.

Durazzo TC, Tosun D, Buckley S, Gazdzinski S, Mon A, Fryer SL, Meyerhoff DJ (2011) Cortical thickness, surface area, and volume of the brain reward system in alcohol dependence: relationships to relapse and extended abstinence. Alcohol Clin Exp Res 35:1187–1200.

Durazzo TC, Mon A, Gazdzinski S, Meyerhoff DJ (2013) Chronic cigarette smoking in alcohol dependence: associations with cortical thickness and N-acetylaspartate levels in the extended brain reward system. Addict Biol 18:379–391.

Durazzo TC, Meyerhoff DJ, Yoder KK (2018) Cigarette smoking is associated with cortical thinning in anterior frontal regions, insula and regions showing atrophy in early Alzheimer's disease. Drug Alcohol Depend 192:277–284.

Duriez Q, Crivello F, Mazoyer B (2014) Sex-related and tissue-specific effects of tobacco smoking on brain atrophy: assessment in a large longitudinal cohort of healthy elderly. Front Aging Neurosci 6:299.

Fein G, Di Sclafani V, Cardenas VA, Goldmann H, Tolou-Shams M, Meyerhoff DJ (2002) Cortical gray matter loss in treatment-naïve alcohol dependent individuals. Alcohol Clin Exp Res 26:558–564.

Fein G, Shimotsu R, Chu R, Barakos J (2009) Parietal gray matter volume loss is related to spatial processing deficits in long-term abstinent alcoholic men. Alcohol Clin Exp Res 33:1806–1814.

Fischl B, Salat DH, Busa E, Albert M, Dieterich M, Haselgrove C, van der Kouwe A, Killiany R, Kennedy D, Klaveness S, Montillo A, Makris N, Rosen B, Dale AM (2002) Whole brain segmentation: automated labeling of neuroanatomical structures in the human brain. Neuron 33:341–355.

Fortier CB, Leritz EC, Salat DH, Venne JR, Maksimovskiy AL, Williams V, Milberg WP, McGlinchey RE (2011) Reduced cortical thickness in abstinent alcoholics and association with alcoholic behavior. Alcohol Clin Exp Res 35:2193–2201.

Glasser MF, Sotiropoulos SN, Wilson JA, Coalson TS, Fischl B, Andersson JL, Xu J, Jbabdi S, Webster M, Polimeni JR, Van Essen DC, Jenkinson M; WU-Minn HCP Consortium (2013) The minimal preprocessing pipelines for the human connectome project. Neuroimage 80:105–124.

Gonzalez-Escamilla G, Lange C, Teipel S, Buchert R, Grothe MJ; Alzheimer's Disease Neuroimaging Initiative (2017) PETPVE12: an SPM toolbox for partial volume effects correction in brain PET - application to amyloid imaging with AV45-PET. Neuroimage 147:669–677.

Haorah J, Ramirez SH, Floreani N, Gorantla S, Morsey B, Persidsky Y (2008) Mechanism of alcohol-induced oxidative stress and neuronal injury. Free Radic Biol Med 45:1542–1550.

Harper C, Kril J, Holloway R (1985) Brain shrinkage in chronic alcoholics: a pathological study. Br Med J (Clin Res Ed) 290:501–504.

Harper C, Kril J, Daly J (1987) Are we drinking our neurones away? Br Med J (Clin Res Ed) 294:534–536.

Henderson KE, Vaidya JG, Kramer JR, Kuperman S, Langbehn DR, O'Leary DS (2018) Cortical thickness in adolescents with a family history of alcohol use disorder. Alcohol Clin Exp Res 42:89–99.

Hindmarsh A (1980) LSODE and LSODI, two new initial value ordinary differnetial equation solvers. ACM SIGNUM Newsletter 15:10–11.

Hommer D, Momenan R, Kaiser E, Rawlings R (2001) Evidence for a gender-related effect of alcoholism on brain volumes. Am J Psychiatry 158:198–204.

Imai K, Keele L, Tingley D (2010) A general approach to causal mediation analysis. Psychol Methods 15:309–334.

Jagannathan NR, Desai NG, Raghunathan P (1996) Brain metabolite changes in alcoholism: an in vivo proton magnetic resonance spectroscopy (MRS) study. Magn Reson Imaging 14:553–557.

Jenkinson M, Bannister P, Brady M, Smith S (2002) Improved optimization for the robust and accurate linear registration and motion correction of brain images. Neuroimage 17:825–841.

Jhala SS, Hazell AS (2011) Modeling neurodegenerative disease pathophysiology in thiamine deficiency: consequences of impaired oxidative metabolism. Neurochem Int 58:248–260.

Kühn S, Schubert F, Gallinat J (2010) Reduced thickness of medial orbitofrontal cortex in smokers. Biol Psychiatry 68:1061–1065.

Lange EH, Nerland S, Jørgensen KN, Mørch-Johnsen L, Nesvåg R, Hartberg CB, Haukvik UK, Osnes K, Melle I, Andreassen OA, Agartz I (2017) Alcohol use is associated with thinner cerebral cortex and larger ventricles in schizophrenia, bipolar disorder and healthy controls. Psychol Med 47:655–668.

Le Berre AP, Rauchs G, La Joie R, Mézenge F, Boudehent C, Vabret F, Segobin S, Viader F, Allain P, Eustache F, Pitel AL, Beaunieux H (2014) Impaired decision-making and brain shrinkage in alcoholism. Eur Psychiatry 29:125–133.

Leenders KL, Perani D, Lammertsma AA, Heather JD, Buckingham P, Healy MJ, Gibbs JM, Wise RJ, Hatazawa J, Herold S (1990) Cerebral blood flow, blood volume and oxygen utilization. Normal values and effect of age. Brain 113:27–47.

Makris N, Oscar-Berman M, Jaffin SK, Hodge SM, Kennedy DN, Caviness VS, Marinkovic K, Breiter HC, Gasic GP, Harris GJ (2008) Decreased volume of the brain reward system in alcoholism. Biol Psychiatry 64:192–202.

Mechtcheriakov S, Brenneis C, Egger K, Koppelstaetter F, Schocke M, Marksteiner J (2007) A widespread distinct pattern of cerebral atrophy in patients with alcohol addiction revealed by voxel-based morphometry. J Neurol Neurosurg Psychiatry 78:610–614.

Meyerhoff DJ, Blumenfeld R, Truran D, Lindgren J, Flenniken D, Cardenas V, Chao LL, Rothlind J, Studholme C, Weiner MW (2004) Effects of heavy drinking, binge drinking, and family history of alcoholism on regional brain metabolites. Alcohol Clin Exp Res 28:650–661.

Momenan R, Steckler LE, Saad ZS, van Rafelghem S, Kerich MJ, Hommer DW (2012) Effects of alcohol dependence on cortical thickness as determined by magnetic resonance imaging. Psychiatry Res 204:101–111.

Müller-Gärtner HW, Links JM, Prince JL, Bryan RN, McVeigh E, Leal JP, Davatzikos C, Frost JJ (1992) Measurement of radiotracer concentration in brain gray matter using positron emission tomography: MRI-based correction for partial volume effects. J Cereb Blood Flow Metab 12:571–583.

Olesen OV, Sullivan JM, Mulnix T, Paulsen RR, Højgaard L, Roed B, Carson RE, Morris ED, Larsen R (2013) List-mode PET motion correction using markerless head tracking: proof-of-concept with scans of human subject. IEEE Trans Med Imaging 32:200–209.

Pfefferbaum A, Lim KO, Zipursky RB, Mathalon DH, Rosenbloom MJ, Lane B, Ha CN, Sullivan EV (1992) Brain gray and white matter volume loss accelerates with aging in chronic alcoholics: a quantitative MRI study. Alcohol Clin Exp Res 16:1078–1089.

Press W, Teukolsky S, Vetterling W, Flannery B (1992) Numerical Recipes in C. The Art of Scientific Computing, 2nd ed. New York: Cambridge University Press.

Raz N, Rodrigue KM (2006) Differential aging of the brain: patterns, cognitive correlates and modifiers. Neurosci Biobehav Rev 30:730–748.

Ritz L, Segobin S, Lannuzel C, Boudehent C, Vabret F, Eustache F, Beaunieux H, Pitel AL (2016) Direct voxel-based comparisons between grey matter shrinkage and glucose hypometabolism in chronic alcoholism. J Cereb Blood Flow Metab 36:1625–1640.

Robbins TW, James M, Owen AM, Sahakian BJ, McInnes L, Rabbitt P (1994) Cambridge neuropsychological test automated battery (CANTAB): a factor analytic study of a large sample of normal elderly volunteers. Dementia 5:266–281.

Schweinsburg BC, Taylor MJ, Alhassoon OM, Videen JS, Brown GG, Patterson TL, Berger F, Grant I (2001) Chemical pathology in brain white matter of recently detoxified alcoholics: a 1H magnetic resonance spectroscopy investigation of alcohol-associated frontal lobe injury. Alcohol Clin Exp Res 25:924–934.

Silveri MM, Cohen-Gilbert J, Crowley DJ, Rosso IM, Jensen JE, Sneider JT (2014) Altered anterior cingulate neurochemistry in emerging adult binge drinkers with a history of alcohol-induced blackouts. Alcohol Clin Exp Res 38:969–979.

Thayer R, Hagerty S, Sabbineni A, Claus E, Hutchison K, Weiland B (2016) Negative and interactive effects of sex, aging, and alcohol abuse on gray matter morphometry. Hum Brain Mapp 2016:6.

Tomasi DG, Shokri-Kojori E, Wiers CE, Kim SW, Demiral ŞB, Cabrera EA, Lindgren E, Miller G, Wang GJ, Volkow ND (2017) Dynamic brain glucose metabolism identifies anti-correlated cortical-cerebellar networks at rest. J Cereb Blood Flow Metab 37:3659–3670.

Volkow ND, Hitzemann R, Wolf AP, Logan J, Fowler JS, Christman D, Dewey SL, Schlyer D, Burr G, Vitkun S (1990) Acute effects of ethanol on regional brain glucose metabolism and transport. Psychiatry Res 35:39–48.

Volkow ND, Wang GJ, Hitzemann R, Fowler JS, Overall JE, Burr G, Wolf AP (1994) Recovery of brain glucose metabolism in detoxified alcoholics. Am J Psychiatry 151:178–183.

Volkow ND, Wang GJ, Overall JE, Hitzemann R, Fowler JS, Pappas N, Frecska E, Piscani K (1997) Regional brain metabolic response to lorazepam in alcoholics during early and late alcohol detoxification. Alcohol Clin Exp Res 21:1278–1284.

Volkow ND, Logan J, Fowler JS, Wang GJ, Gur RC, Wong C, Felder C, Gatley SJ, Ding YS, Hitzemann R, Pappas N (2000) Association between age-related decline in brain dopamine activity and impairment in frontal and cingulate metabolism. Am J Psychiatry 157:75–80.

Volkow ND, Wang GJ, Franceschi D, Fowler JS, Thanos PP, Maynard L, Gatley SJ, Wong C, Veech RL, Kunos G, Kai Li T (2006) Low doses of alcohol substantially decrease glucose metabolism in the human brain. Neuroimage 29:295–301.

Volkow ND, Ma Y, Zhu W, Fowler JS, Li J, Rao M, Mueller K, Pradhan K, Wong C, Wang GJ (2008) Moderate doses of alcohol disrupt the functional organization of the human brain. Psychiatry Res 162:205–213.

Volkow ND, Kim SW, Wang GJ, Alexoff D, Logan J, Muench L, Shea C, Telang F, Fowler JS, Wong C, Benveniste H, Tomasi D (2013) Acute alcohol intoxication decreases glucose metabolism but increases acetate uptake in the human brain. Neuroimage 64:277–283.

Volkow ND, Wang GJ, Shokri Kojori E, Fowler JS, Benveniste H, Tomasi D (2015) Alcohol decreases baseline brain glucose metabolism more in heavy drinkers than controls but has no effect on stimulation-induced metabolic increases. J Neurosci 35:3248–3255.

Volkow ND, Wiers CE, Shokri-Kojori E, Tomasi D, Wang GJ, Baler R (2017) Neurochemical and metabolic effects of acute and chronic alcohol in the human brain: studies with positron emission tomography. Neuropharmacology 122:175–188.

Wang GJ, Volkow ND, Roque CT, Cestaro VL, Hitzemann RJ, Cantos EL, Levy AV, Dhawan AP (1993) Functional importance of ventricular enlargement and cortical atrophy in healthy subjects and alcoholics as assessed with PET, MR imaging, and neuropsychologic testing. Radiology 186:59–65.

Wang GJ, Volkow ND, Franceschi D, Fowler JS, Thanos PK, Scherbaum N, Pappas N, Wong CT, Hitzemann RJ, Felder CA (2000) Regional brain metabolism during alcohol intoxication. Alcohol Clin Exp Res 24:822–829.

Wang GJ, Volkow ND, Fowler JS, Franceschi D, Wong CT, Pappas NR, Netusil N, Zhu W, Felder C, Ma Y (2003) Alcohol intoxication induces greater reductions in brain metabolism in male than in female subjects. Alcohol Clin Exp Res 27:909–917.

Zahr NM, Pfefferbaum A (2017) Alcohol's effects on the brain: neuroimaging results in humans and animal models. Alcohol Res 38:183–206.

Zeileis A (2006) Object-oriented computation of sandwich estimators. J Stat Softw 16:1–16.